Global Energy Interconnection
Development and Cooperation Organization

ELSEVIER
Production And Hosting By Elsevier On Behalf Of KeAi
KeAi

Volume 6 Number 6 December 2023 (700-713)
DOI: 10.1016/j.gloei.2023.12.004

Global Energy Interconnection

Contents lists available at ScienceDirect
https: //www.sciencedirect.com/journal/global-energy-interconnection

Full-length article

Coordinated planning for flexible interconnection and energy storage system in low-voltage distribution networks to improve the accommodation capacity of photovoltaic

Jiaguo Li[1], Lu Zhang[1], Bo Zhang[1], Wei Tang[1]

1. College of Information and Electrical Engineering, China Agricultural University, Beijing 100083, P. R. China

Scan for more details

Abstract: The increasing proportion of distributed photovoltaics (DPVs) and electric vehicle charging stations in low-voltage distribution networks (LVDNs) has resulted in challenges such as distribution transformer overloads and voltage violations. To address these problems, we propose a coordinated planning method for flexible interconnections and energy storage systems (ESSs) to improve the accommodation capacity of DPVs. First, the power-transfer characteristics of flexible interconnection and ESSs are analyzed. The equipment costs of the voltage source converters (VSCs) and ESSs are also analyzed comprehensively, considering the differences in installation and maintenance costs for different installation locations. Second, a bilevel programming model is established to minimize the annual comprehensive cost and yearly total PV curtailment capacity. Within this framework, the upper-level model optimizes the installation locations and capacities of the VSCs and ESSs, whereas the lower-level model optimizes the operating power of the VSCs and ESSs. The proposed model is solved using a non-dominated sorting genetic algorithm with an elite strategy (NSGA-II). The effectiveness of the proposed planning method is validated through an actual LVDN scenario, which demonstrates its advantages in enhancing PV accommodation capacity. In addition, the economic benefits of various planning schemes with different flexible interconnection topologies and different PV grid-connected forms are quantitatively analyzed, demonstrating the adaptability of the proposed coordinated planning method.

Keywords: Low-voltage distribution network; Photovoltaic accommodation; Flexible interconnection; Energy storage system; Bilevel programming

0 Introduction

With the proposal of carbon peaking and carbon neutrality goals, the proportion of renewable energy represented by distributed photovoltaics (DPVs) in distribution networks will increase significantly. Additionally, the proportion of the DC load represented by electric vehicle charging stations is constantly increasing, resulting in complex and variable power supply and load characteristics of low-voltage distribution networks (LVDNs). In this context, the conventional radial operation mode of an AC distribution network is no longer applicable because of the lack of flexibility. On one hand, overvoltage

Received: 17 July 2023/Revised: 13 September 2023/Accepted: 13 October 2023/Published: 25 December 2023

✉ Wei Tang
wei_tang@cau.edu.cn

Lu Zhang
zhanglu1@cau.edu.cn

Jiaguo Li
li_jiaguo@foxmail.com

Bo Zhang
zhangbo1223@foxmail.com

problems may occur because of the high proportion of DPV integration, and network losses may also increase because of the reverse power from the LVDN to the medium-voltage distribution network (MVDN) [1-3]. On the other hand, the peak load period of electric vehicle charging stations may be the same as that of conventional loads, exacerbating the overload of the distribution transformer [4, 5]. Therefore, enhancing the accommodation capacity of LVDNs and mitigating power quality problems caused by the integration of PVs and electric vehicle charging stations are important.

The conventional approach to these challenges involves enhancing the distribution network. Nevertheless, the significant upgrades and reconstruction of both primary and secondary equipment can entail longer construction timelines and considerable investments. Furthermore, the utilization efficiency of the upgraded equipment remains relatively modest owing to the short occurrence time of reverse power and the overload problem of distribution transformers. The reactive power regulation capability of PV inverters can be used to alleviate the overvoltage problems in distribution networks with a high proportion of PVs [6]. A distributed reactive power compensation method connecting single-phase DPV inverters to different phases was proposed in [7]. However, this method cannot manage the actual power imbalance between the supply and demand sides even when the overvoltage problem can be alleviated. In addition, conventional AC distribution networks achieve power transfer by changing the state of the interconnection switches; however, their performance within a short period is limited [8]. In response, scholars have proposed the concept of flexible interconnection as a replacement for conventional switches, thereby effectively accommodating PVs through flexible power transfer [9-11].

Notably, a voltage source converter (VSC)-based flexible interconnection is a more cost-effective option than power electronic transformers, making it particularly suitable for LVDNs. The operational characteristics of flexible interconnection devices were analyzed in [12, 13], which achieved accurate and reliable real-time power control. Reference [14] analyzed the maximum power-supply capacity of a distribution network by considering the flexible interconnection of low-voltage distribution areas. Reference [15] optimized the capacity and position of VSCs to mitigate the voltage violation and overload problem of distribution transformers by considering the power complementarity between the DC and AC lines. The UK Grid Corporation initiated the FUN-LV project in 2014, demonstrating commendable economic, social, and environmental gains [16]. Nonetheless, the application of flexible DC technology for achieving load balancing, fault load restoration, and supply-demand interaction is in its nascent stages, and application experience is lacking. Flexible interconnections in different regions cannot be adopted in fixed standard mode [17]. Moreover, owing to the inconsistency between the peak period of PV power generation and that of load electricity consumption, the power emitted by a PV system may far exceed the total load electricity demand of the two areas simultaneously. The use of only flexible interconnections between distribution areas with a high proportion of PVs may not achieve complete PV accommodation.

Furthermore, some scholars have demonstrated that the accommodation capacity of PV can be improved by configuring energy storage systems (ESSs) [18-20]. Reference [21] indicated that increasing the accommodation capacity of renewable energy by allocating ESSs is a trend in intelligent distribution networks. Reference [22] proposed an optimization scheduling model based on mobile ESS that effectively mitigates the overvoltage problem caused by the large-scale integration of distributed generation and household electric vehicles in distribution networks. Reference [23] utilized distributed ESS devices to mitigate the adverse effects of PV integration, distributed ESS planning, and operation techniques, and accurately calculated the power value of PV that violates system constraints. Reference [24] proposed a large-scale multi-ESS combination application scheme based primarily on NaS batteries for renewable energy consumption. However, various ESS battery technologies have their limitations, and their investment costs remain relatively high [25]. With an increasing proportion of DPVs, relying solely on configuring the ESS may not guarantee economy.

The coordinated planning of flexible interconnections and ESS for LVDNs can fully utilize the spatiotemporal power-transfer capacity, which is significant for improving PV accommodation. Numerous research achievements have been made in scheduling. A collaborative scheduling strategy based on a VSC and ESS that utilizes spatiotemporal power transfer was proposed to demonstrate its superiority in PV accommodation [26]. Reference [27] proposed a two-level scheduling algorithm to address voltage regulation by coordinating customer-owned ESS and utility-owned load tap changers in power distribution systems. Few research achievements have been attained in terms of planning. Reference [28] established a collaborative planning model for the location and capacity of ESS and DC lines to achieve high-quality and cost-effective accommodation of PVs within and between regions. Reference [29] proposed a planning approach for the network configuration of AC-DC hybrid distribution systems. However, power losses were

not considered, or quantitative analysis of various flexible interconnection topologies and different PV grid-connected forms was lacking [28, 29].

The existing planning methods for LVDNs have several limitations. First, they fail to exploit the advantages of flexible interconnection devices and ESSs fully. While an ESS may achieve full PV accommodation, relying solely on configuring the ESS can result in higher investment costs. Conversely, flexible interconnection may not achieve full PV accommodation; however, it has a lower investment cost [14]. Previous studies focused on either configuring ESSs or flexible interconnection devices to enhance PV accommodation. Furthermore, current dual-layer optimization models do not consider differences in investment costs among various interconnection points or disparities in maintenance costs for newly added equipment in different locations. Additionally, the economy of planning schemes with different flexible interconnection topologies and different PV grid-connected forms has not been analyzed quantitatively. With the increasing proportion of DPVs, coordinated planning for flexible interconnection and ESS is necessary to achieve an equilibrium between the economy and PV accommodation.

The main contributions of this work are as follows:

1) A bilevel coordinated planning model of flexible interconnection devices and ESSs for LVDNs, considering the power-transfer characteristics in both spatial and temporal dimensions, is established. The model considers the differences in investment costs for different interconnected locations and refines the formulation of equipment maintenance costs.

2) The economies of various planning schemes with different flexible interconnection topologies and different PV grid-connected forms are quantitatively analyzed, demonstrating the adaptability of the proposed coordinated planning method.

The remainder of this paper is organized as follows. Section 1 analyzes the power-transfer characteristics of flexible interconnection devices and ESSs. Section 2 analyzes economic costs. Section 3 establishes a bilevel programming model with two objective functions. Section 4 presents simulation results. Finally, Section 5 presents the conclusions of this study.

1 Analysis of power-transfer characteristics of flexible interconnection and ESS

Owing to the temporal and spatial differences in the power distribution between the DPVs and loads in LVDNs, the integration of DPVs may result in overvoltage and reverse power. To mitigate these problems and improve the accommodation capacity of PVs, we must analyze the power-transfer characteristics of flexible interconnection devices and ESSs.

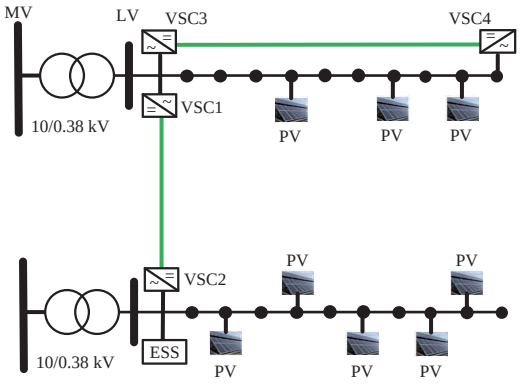

Fig. 1 LVDNs with flexible interconnection devices and ESSs

1.1 Power-transfer characteristics based on flexible interconnections

Flexible interconnection devices enable power transmission between two regions. Flexible interconnections can be broadly divided into three topologies: interconnections among front nodes, terminal nodes, and intermediate nodes. Flexible interconnections facilitate electricity transmission between distribution areas, thus alleviating distribution transformer overloads. In addition, a parallel connection exists within the distribution area, and the DC and AC lines are installed on the same electric power tower, such as VSC3 and VSC4 in Fig. 1. Based on the background of actual engineering construction, this topology may be adopted when flexible interconnection devices and allocation of the ESS fail to mitigate voltage violations.

The control modes of VSC may be classified into $V_{dc}-\theta$ control, $V_{dc}-Q$ control, $V_{dc}-V_{ac}$ control, $P-Q$ control, etc. [30]. For the hybrid AC–DC distribution network shown in Fig. 1, the main function of VSC1 and VSC3 is to stabilize the DC voltage; therefore, $V_{dc}-Q$ control mode is adopted. VSC4 and VSC2 are used to transfer active and reactive powers between the two sides of VSCs, thus achieving flexible control of the power flow. Therefore, the $P-Q$ control mode is adopted.

The power balance constraint must be satisfied on both sides when the VSC operates. The total active power injected into the VSC on the AC side should equal the active power output on the DC side. Additionally, the active and reactive power outputs of the VSC must satisfy its capacity

constraints, as expressed by the following equations:

$$P_{VSC,t}^{AC} = -P_{VSC,t}^{DC} \tag{1}$$

$$P_{VSC,t}^{AC\ 2} + Q_{VSC,t}^{AC\ 2} \leqslant S_{VSC}^{2} \tag{2}$$

where $P_{VSC,t}^{AC}$ and $Q_{VSC,t}^{AC}$ are the active and reactive powers of the VSC on the AC side at time *t*, respectively; $P_{VSC,t}^{DC}$ is the active power on the DC side at time *t*; S_{VSC} represents the capacity of the VSC.

1.2 Power-transfer characteristics based on an ESS

An ESS may achieve power transfer over a temporal scale and facilitate economically stable operations through peak-shaving and valley-filling strategies. In this paper, coordinated scheduling of the ESS and VSC is employed to achieve spatial and temporal power transmission.

First, the charging and discharging powers of the ESS cannot exceed the power limit when the ESS operates. Second, the state of charge (SOC) of the ESS changes with charging and discharging cycles. The SOC should be maintained between 20% and 80% of its maximum capacity to ensure the longevity of the ESS [31]. Finally, the SOC at the end of each scheduling day must be equal to the SOC at the beginning of the scheduling day to maintain cyclic scheduling.

$$\begin{cases} 0 \leqslant P_{ESSch}(t) \leqslant P_{ESSch,\max} \\ 0 \leqslant P_{ESSdis}(t) \leqslant P_{ESSdis,\max} \end{cases} \tag{3}$$

$$SOC_{ESS}(t) = SOC_{ESS}(t-1) + SOC_{ESS}(\Delta t) \tag{4}$$

$$SOC_{ESS}(\Delta t) = \begin{cases} \lambda_1 P_{ESSch}(t)\eta_{ESSch}\Delta t \\ \lambda_2 \dfrac{-P_{ESSdis}(t)\Delta t}{\eta_{ESSdis}} \end{cases} \tag{5}$$

$$\lambda_1 + \lambda_2 \leqslant 1, \forall t \tag{6}$$

$$SOC_{ESS\min} \leqslant SOC_{ESS}(t) \leqslant SOC_{ESS\max} \tag{7}$$

$$SOC_{ESS,j,T_{\text{bejin}}} = SOC_{ESS,j,T_{finish}} \tag{8}$$

where $P_{ESSch}(t)$ and $P_{ESSdis}(t)$ are the charging and discharging powers of the ESS at time *t*, respectively; $P_{ESSch,\max}$ and $P_{ESSdis,\max}$ are the maximum charging and discharging powers of the ESS, respectively; $SOC_{ESS}(t)$, $SOC_{ESS}(t-1)$ are the SOCs of the ESS at time t and *t*−1, respectively; $SOC_{ESS}(\Delta t)$ is the change in the SOC over time; λ_1 and λ_2 are binary variables that represent the charging and discharging states of the ESS, respectively; η_{ESSch} and η_{ESSdis} are the charging and discharging efficiencies of the ESS; $SOC_{ESS\min}$ and $SOC_{ESS\max}$ are the minimum and maximum SOC values of the ESS, respectively; $SOC_{ESS,j,T_{\text{bejin}}}$ and $SOC_{ESS,j,T_{finish}}$ are the SOCs at the beginning and end of daily scheduling for the ESS at node *j*, respectively.

2 Economic cost analysis of flexible interconnection devices and ESS

Economic viability is a crucial factor in the planning of LVDNs. Therefore, before the planning process, the costs associated with the equipment must be analyzed.

In terms of investment costs, previous studies primarily focused on the investment costs of VSC, ESS, and new DC lines. However, the construction level of the front nodes is relatively high, typically featuring a distribution box that facilitates the connection of the DC side of the VSC to the DC line, thereby providing interconnection conditions. By contrast, the power towers of the other nodes are equipped with lines without distribution boxes. Distribution boxes must be added to facilitate the connection between the DC side of the VSC and the DC line. Therefore, this paper considers the additional investment costs incurred by adding distribution boxes.

In terms of operation and maintenance costs, previous studies primarily focused on line loss, operational loss of new equipment, and load-shedding costs. However, because of the integration of new devices in the LVDN, grid companies must allocate personnel for regular inspections and maintenance, incurring labor and maintenance material costs. The costs of single maintenance of the ESS and VSC are expressed as C_{ESS}^{ser} and C_{VSC}^{ser}, respectively. The voltage level of the newly added DC lines is low and the interconnection distance is short, making their maintenance costs essentially negligible. Additionally, because the new equipment requires annual maintenance assistance from power equipment manufacturers, the grid company must pay additional annual maintenance fees to these manufacturers, denoted as C_{ESS}^{vender} and C_{VSC}^{vender}. Reference [32] approximated the maintenance costs as a certain proportion of the annual equipment investment costs. However, considering factors such as the topography and traffic conditions of an actual LVDN, the timing of equipment maintenance varies at different locations. Therefore, the one-time maintenance costs for the equipment also differ according to location. This is particularly relevant when new equipment is connected to the end of the distribution areas, where it might be less convenient for inspection personnel to perform maintenance. Additionally, external environmental conditions can significantly affect the operation of electrical equipment, resulting in different operating states for electrical equipment at various locations [33]. Operational

and maintenance costs may vary with different equipment states [34]. Moreover, from a safety perspective, if an ESS is not connected to a front node, the frequency of maintenance events may increase, particularly when the ESS is connected to nodes with a significant number of users. Therefore, this paper refines the mathematical model for maintenance costs, as shown in (9).

$$\begin{cases} C_{ESS}^{ser} = \sum_{j=1}^{N_{ESS}} \sum_{n=1}^{N_{ESS,j}^{ser}} C_{ESS,n,j} \\ C_{VSC}^{ser} = \sum_{i=1}^{N_{VSC}} \sum_{n=1}^{N_{VSC,i}^{ser}} C_{VSC,n,i} \\ C_{ESS}^{vender} = \dfrac{\sum_{y=1}^{Y_{ESS}} \sum_{j=1}^{N_{ESS}} a_{ESS,y}^{vender} S_{ESS,j}}{Y_{ESS}} \\ C_{VSC}^{vender} = \dfrac{\sum_{y=1}^{Y_{VSC}} \sum_{i=1}^{N_{VSC}} a_{VSC,y}^{vender} S_{VSC,i}}{Y_{VSC}} \end{cases} \tag{9}$$

where C_{ESS}^{ser} and C_{VSC}^{ser} are the annual inspection and maintenance costs of the power grid companies of the ESS and VSC, respectively; C_{ESS}^{vender} and C_{VSC}^{vender} are the additional annual maintenance fees of the ESS and VSC paid by the grid companies, respectively; $N_{ESS,j}^{ser}$ is the total number of annual inspections of the ESS located at node j; $N_{VSC,i}^{ser}$ is the total number of annual inspections of VSC located at node i; $C_{ESS,n,j}$ and $C_{VSC,n,i}$ are the single maintenance costs for the ESS and VSC, respectively; Y_{ESS} and Y_{VSC} are the depreciation years for the ESS and VSC, respectively. $S_{ESS,j}$ is the capacity of the ESS at node j; $S_{VSC,i}$ is the capacity of the VSC at node i; $a_{ESS,y}^{vender}$ and $a_{VSC,y}^{vender}$ are the unit capacity regular maintenance costs for year y of the ESS and VSC, respectively; $a_{ESS,y}^{vender}$ and $a_{VSC,y}^{vender}$ are 0 during the warranty period.

In summary, this section comprehensively considers the practicalities of project construction and factors influencing maintenance costs. This section proposes the investment cost of newly added distribution boxes and analyzes the impact of the different locations of newly added equipment on maintenance costs.

3 Planning model

Flexible interconnection devices and ESSs enhance the accommodation capacity of PVs. Although flexible interconnection devices have lower investment costs, they lack a fixed standard mode across different regions, resulting in varying PV accommodation capacities. Despite ESS allocation significantly increasing the PV accommodation capacity, its higher investment costs and shorter depreciation period than a VSC must be considered. The rational planning of flexible interconnection devices and ESS must consider both economic feasibility and PV accommodation capacity. Thus, this paper establishes a bilevel programming model based on flexible interconnection devices and an ESS.

3.1 Upper-level planning model

From the perspective of a power grid company, this paper optimizes the installation locations and capacities of VSCs and ESSs in upper-level planning. The objective function aims to minimize the annual comprehensive cost and total PV curtailment power capacity per year. Because new DC lines must be constructed for the interconnection between VSCs, the cost of the DC lines is already included in the annual investment costs.

(1) Objective function

The upper-level planning model establishes objective functions to minimize the annual comprehensive cost and total PV curtailment power capacity per year:

$$\min F_1 = C_{inv}^{S} + C_o \tag{10}$$

$$\min F_2 = 365 \sum_{t=1}^{T_{\max}} \sum_{i \in N_{DN}} (P_{PVgen,i,t} - P_{PVnet,i,t}) \Delta t \tag{11}$$

where C_{inv}^{S} represents the annual investment cost of the VSC, ESS, DC lines, and newly added distribution boxes; C_o represents the annual operation and maintenance cost obtained from the lower-level optimization model; $T_{\max}$ represents the number of time nodes, which is 24 h; N_{DN} represents a collection of nodes in the LVDN; $P_{PVgen,i,t}$ and $P_{PVnet,i,t}$ represent the PV output and grid-connected power of node i at time t, respectively; Δt is the length of the period.

$$C_{inv}^{S} = \sum_{i=1}^{N_{VSC}} \alpha_{VSC} C_{VSC} S_{VSC,i} + \sum_{j=1}^{N_{ESS}} \alpha_{ESS} C_{ESS} S_{ESS,j} + \alpha_L C_L L_{DC} + \alpha_{DB} C_{DB} N_{DB} \tag{12}$$

where N_{VSC} and M_{ESS} represent the total number of VSCs and ESSs, respectively; C_{VSC} and C_{ESS} are the unit capacity investment costs for the VSC and ESS, respectively; C_L is the investment cost per unit length of the DC line. C_{DB} is the investment cost of a distribution box. $S_{VSC,i}$ is the installation capacity of the VSC at node i; $S_{ESS,j}$ is the installation capacity of the ESS at node j; L_{DC} is the total length of the DC lines; N_{DB} is the total number of newly added distribution boxes; α_{VSC}, α_{ESS}, α_L, and α_{DB} are the annual average cost coefficients of fixed investments for VSC, ESS, DC lines, and distribution boxes, respectively.

$$\alpha = \frac{r(1+r)^Y}{(1+r)^Y - 1} \tag{13}$$

where r is the discount rate, and Y is the depreciation period of the equipment.

Considering the differences in the maintenance costs of newly added equipment at different locations, the maintenance cost model established in this paper is expressed as follows:

$$C_o = C_{loss} + C_{device} + C_{service} + C_{load} \tag{14}$$

where C_{loss} represents the annual cost of line loss, C_{device} represents the annual operating costs for the VSC and ESS, $C_{service}$ represents the annual maintenance costs for the VSC and ESS; C_{load} represents the annual load-shedding cost.

$$C_{loss} = 365\sum_{t=1}^{T_{\max}} C_e \left(\sum_{l\in\Omega_{AC,line}} P_{AC,L,t,l} + \sum_{l\in\Omega_{DC,line}} P_{DC,L,t,l} \right)\Delta t \tag{15}$$

where C_e is the real-time electricity price; $P_{AC,L,t,l}$ and $P_{DC,L,t,l}$ represent the line losses during time t in the AC and DC systems, respectively; $\Omega_{AC,line}$ and $\Omega_{DC,line}$ are the collections of branches for AC and DC systems, respectively.

$$C_{device} = 365\sum_{t=1}^{T_{\max}} \left(a_{VSC,i} \sum_{i=1}^{N_{VSC}} P_{VSC,t,i} + a_{ESS,j} \sum_{j=1}^{N_{ESS}} P_{ESS,t,j} \right)\Delta t \tag{16}$$

where $a_{VSC,i}$ and $a_{ESS,j}$ are the unit operating costs of the VSC and ESS, respectively; $P_{VSC,t,i}$ and $P_{ESS,t,j}$ are the active power outputs of the VSC and ESS, respectively.

$$C_{service} = C_{ESS}^{ser} + C_{VSC}^{ser} + C_{ESS}^{vender} + C_{VSC}^{vender} \tag{17}$$

$$C_{load} = 365C_l \sum_{t=1}^{T_{\max}} \sum_{i\in\Omega_{load,t}} P_{in,t,i}\Delta t \tag{18}$$

where C_l is the penalty cost for unit load shedding, $P_{in,t,i}$ is the active power value of the load located at node i during period t, and $\Omega_{load,t}$ is the set of nodes in which load shedding occurs during period t.

(2) Constraints

The upper-level planning model primarily considers constraints related to equipment investment costs and aims to satisfy the constraint of maximizing investment costs:

$$C_{inv}^{S} \leqslant C_{inv,\max}^{S} \tag{19}$$

where $C_{inv,\max}^{S}$ represents the maximum allowable value of the total investment cost of the equipment.

3.2 Lower-level optimization model

The lower-level optimization model aims to minimize the annual operation and maintenance costs and the total PV curtailment power capacity per year. Based on the installation locations and capacities of the VSCs and ESS provided by the upper-level planning model, the power outputs of the ESS and VSCs are optimized. Subsequently, the power values are fed back to the upper-level planning model to accurately calculate the objective function value and continue the optimization process.

(1) Objective function

The objective is to minimize the annual operation and maintenance costs and the total PV curtailment capacity per year to the greatest extent possible.

$$\min f_1 = C_o \tag{20}$$

$$\min F_2 = 365\sum_{t=1}^{T_{\max}} \sum_{i\in N_{\mathrm{DN}}} (P_{PVgen,i,t} - P_{PVnet,i,t})\Delta t \tag{21}$$

(2) Constraints

1) Power flow equation constraints

$$\begin{cases} P_i^{PV} + P_i^{VSC} + P_i^{ESS} - P_i^{load} = \\ U_i \sum_{j=1}^{n} U_j (G_{ij}\cos\delta_{ij} + B_{ij}\sin\delta_{ij}) \\ Q_i^{PV} + Q_i^{VSC} + Q_i^{ESS} - Q_i^{load} = \\ U_i \sum_{j=1}^{n} U_j (G_{ij}\sin\delta_{ij} - B_{ij}\cos\delta_{ij}) \end{cases} \tag{22}$$

where P_i^{PV} and Q_i^{PV} represent the active and reactive powers injected by the PV at node i, respectively; P_i^{VSC} and Q_i^{VSC} represent the active and reactive powers injected by the VSC at node i, respectively; P_i^{ESS} and Q_i^{ESS} represent the active and reactive powers injected by ESS at node i, respectively; P_i^{load} and Q_i^{load} represent the active and reactive loads of node i, respectively; G_{ij}, B_{ij}, and δ_{ij} represent the conductivity, admittance, and voltage phase between nodes i and j, respectively; n is the total number of nodes; U_i and U_j are the voltage amplitudes of nodes i and j.

2) Node voltage constraints

For each node in the LVDN, the voltage amplitude cannot exceed the upper voltage limit or fall below the lower limit. The range is 93%–107% of the standard voltage.

$$U_{i,\min} \leqslant U_i \leqslant U_{i,\max} \tag{23}$$

where $U_{i,\min}$ and $U_{i,\max}$ are the minimum and maximum values of node i, respectively.

3) Branch power constraint

The VSC transmits power through interconnected lines, and the sum of its power and the original load power of the line cannot exceed the capacity of the line.

$$\begin{cases} (P_{VSC,t}^{AC} + P_{LOAD,t}^{AC})^2 + (Q_{VSC,t}^{AC} + Q_{LOAD,t}^{AC})^2 \leqslant S_{AC}^2 \\ P_{VSC,t}^{DC} + P_{LOAD,t}^{DC} \leqslant S_{DC} \end{cases} \tag{24}$$

where $P_{VSC,t}^{AC}$, $Q_{VSC,t}^{AC}$, and $P_{VSC,t}^{DC}$ represent the power of the VSC on both sides; $P_{LOAD,t}^{AC}$, $Q_{LOAD,t}^{AC}$, and $P_{LOAD,t}^{DC}$ represent the load powers of AC and DC distribution networks, respectively; S_{AC} and S_{DC} represent the capacities of the AC and DC lines, respectively.

4) Constraints on the reverse power

The objective of the bilevel programming model is to enhance the accommodation capacity of the PV; therefore, we must ensure that the reverse power cannot be transferred from the LVDN to the MVDN [14]. The specific constraints are as follows:

$$P_{0,t}^{AC} \geqslant 0, t \in [1, T_{\max}] \tag{25}$$

where $P_{0,t}^{AC}$ represents the outlet power of the distribution transformer at time t.

5) ESS capacity constraints

$$-S_{ESS,j} \leqslant P_{ESS,j,t} \leqslant S_{ESS,j} \tag{26}$$

where $P_{ES,j,t}$ is the active power of the ESS at node j.

6) VSC capacity constraint

The constraint on VSC capacity is represented by (2). Moreover, the operational loss of the VSC is considered. The VSC loss rate should not exceed the maximum permissible loss rate.

$$\xi_t^{VSC} \leqslant \xi_{\max}^{VSC} \tag{27}$$

where ξ_t^{VSC} and $\xi_{\max}^{VSC}$ refer to the VSC loss rate at time t and the maximum allowable loss rate, respectively.

In addition, considering the distribution transformer overloads, the distribution transformer must satisfy the following constraints:

$$P^L(t) \geqslant 0 \tag{28}$$

$$\sqrt{P^H(t)^2 + Q^H(t)^2} \leqslant 0.7 S_T \tag{29}$$

where $P^L(t)$ is the active power on the low-voltage side of the distribution transformer at time t; $P^H(t)$ and $Q^H(t)$ are the active and reactive powers on the high-voltage side of the distribution transformer at time t, respectively; S_T is the capacity of the distribution transformer.

3.3 Solution method

To enhance computational efficiency, this study established an LVDN model based on the CloudPSS-IESLab2 platform to establish candidate position sets for the VSC and ESS. Subsequently, a non-dominated sorting genetic algorithm with an elite strategy (NSGA-II), which may solve the equilibrium between economy and PV accommodation, was used to solve the proposed bilevel programming model. NSGA-II uses an elite retention strategy, which is a multi-objective optimization algorithm based on Pareto optimal solutions. The upper-level model divides chromosomes into several segments, representing candidate positions for multiple VSCs and ESSs, and uses binary encoding based on chromosome length to represent the capacity of the VSCs and ESSs. The lower-level model optimizes the power of the VSCs and ESSs to obtain the optimal operational state of the LVDN, and the results are then fed back to the upper-level model.

In genetic operations, an improved genetic algorithm that combines the termination evolution criteria of the optimal retention strategy, adaptive crossover rate, mutation rate, and optimal individual minimum retention algebra with the maximum genetic algebra is used to obtain a globally optimal solution.

4 Simulation analysis

4.1 Background of the case

Based on the actual LVDN, the initial parameters, such as lines and loads, were set up on the MATLAB platform. Figure 2 shows the original structure of the AC distribution network. The 24-h curves of the PV and load are shown in Fig. 3. All nodes (excluding node 0) in area 1 installed DPVs with the same capacity, and the PV penetration rate in area 1 was 147.4%. The load parameters for each node in areas 1 and 2 remained consistent throughout a typical day, and the power factor of all loads was set to 0.99.

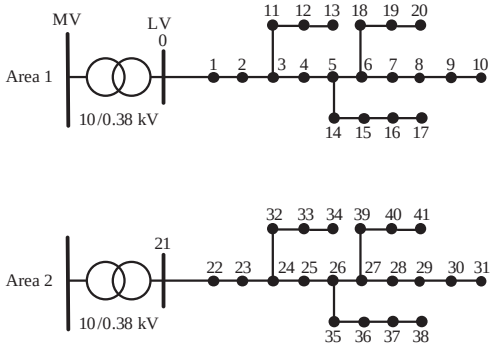

Fig. 2 Original AC LVDN

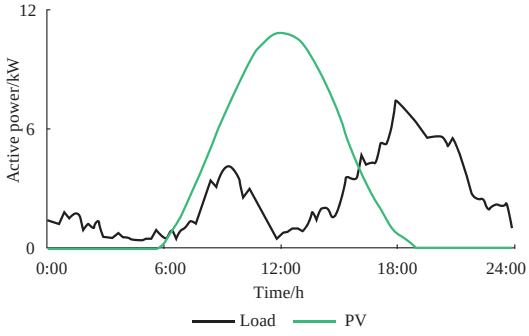

Fig. 3 24-hour curves of PV and load

The rated capacities of the dual winding transformer in areas 1 and 2 were set to 0.3 and 0.15 MVA, respectively. The line model for both areas 1 and 2 was LGJ-70, and the line resistance parameters are listed in Table 1.

Table 2 lists some parameter values used to solve the bilevel programming model. Additionally, based on the actual terrain of area 1, nodes 0–6 were assumed to be located along well-connected main roads, whereas the other nodes were on branch roads with poor road conditions. The total number of annual inspections $N_{ES,j}^{ser}$ and the single maintenance cost (yuan) $C_{ES,n,j}$ are shown in the following equations:

$$N_{ES,j}^{ser} = \begin{cases} 12, j = 0,1,2 \\ 18, j = others \end{cases} \tag{30}$$

Table 1 Line resistance parameters

Line	Length/km	Impedance/Ω	Line	Length/km	Impedance/Ω
0-1	0.022	0.0101+j0.0088	22-23	0.022	0.0101+j0.0088
1-2	0.022	0.0101+j0.0088	23-24	0.022	0.0101+j0.0088
2-3	0.022	0.0101+j0.0088	24-25	0.022	0.0101+j0.0088
3-4	0.022	0.0101+j0.0088	25-26	0.022	0.0101+j0.0088
4-5	0.022	0.0101+j0.0088	26-27	0.022	0.0101+j0.0088
5-6	0.022	0.0101+j0.0088	27-28	0.022	0.0101+j0.0088
6-7	0.022	0.0101+j0.0088	28-29	0.022	0.0101+j0.0088
7-8	0.022	0.0101+j0.0088	29-30	0.022	0.0101+j0.0088
8-9	0.022	0.0101+j0.0088	30-31	0.022	0.0101+j0.0088
9-10	0.022	0.0101+j0.0088	24-32	0.014	0.0064+j0.0056
3-11	0.014	0.0064+j0.0056	32-33	0.014	0.0064+j0.0056
11-12	0.014	0.0064+j0.0056	33-34	0.014	0.0064+j0.0056
12-13	0.014	0.0064+j0.0056	26-35	0.014	0.0064+j0.0056
5-14	0.014	0.0064+j0.0056	35-36	0.014	0.0064+j0.0056
14-15	0.014	0.0064+j0.0056	36-37	0.014	0.0064+j0.0056
15-16	0.014	0.0064+j0.0056	37-38	0.014	0.0064+j0.0056
16-17	0.014	0.0064+j0.0056	27-39	0.014	0.0064+j0.0056
6-18	0.014	0.0064+j0.0056	39-40	0.014	0.0064+j0.0056
18-19	0.014	0.0064+j0.0056	40-41	0.014	0.0064+j0.0056
19-20	0.014	0.0064+j0.0056	0-21	0.4	\
21-22	0.022	0.0101+j0.0088	10-31	0.4	\

Table 2 Partial parameter values

Parameter	Value
Unit capacity ESS investment/(yuan/kWh)	3000
VSC investment per unit capacity/(yuan/kVA)	1000
DC line investment per unit length/(yuan/m)	220
Depreciation period of ESS/year	8
Depreciation period of VSC/year	20
Depreciation period of DC lines/year	20
Unit electricity price/(yuan/kVA)	0.55
Discount rate/%	10
Investment for a single distribution box/yuan	2000
Depreciation period of distribution box/year	20

$$C_{ES,n,j}=\begin{cases}300, j=0,1,\quad,6\\450, j=others\end{cases} \tag{31}$$

The phenomenon of reverse power in area 1 was severe at noon, as shown in Fig. 4. The power generated by a PV system exceeded the electricity demand because this was the peak period of PV power generation. Area 2 experienced an overload problem with the distribution transformer in the evening. This was because of the smaller capacity of the transformer in area 2, which coincided with the peak period of electricity demand.

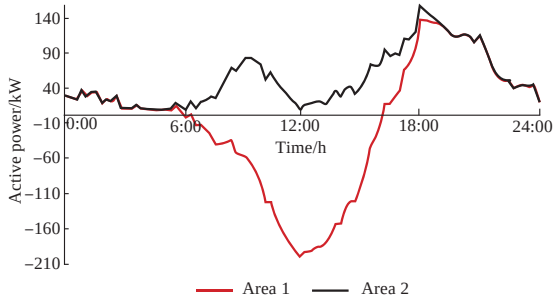

Fig. 4 Power of slack bus in areas 1 and 2

The remainder of this section is organized as follows: Section 4.2 provides a verification and comparison of

coordinated planning methods, thereby validating their advantages in enhancing PV accommodation capacity. Sections 4.3 and 4.4 analyze the economy of planning schemes with different flexible interconnection topologies and different PV grid-connected forms, demonstrating the adaptability of the proposed coordinated planning method.

4.2 Verification and analysis of coordinated planning methods

NSGA-II was used to solve the problem using the proposed bilevel programming model. The decision variables were the installation locations and capacities of the VSCs and ESS. The site selection results for the VSCs and ESS are shown in Fig. 5.

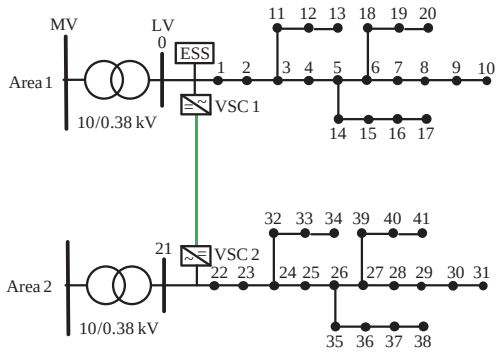

Fig. 5 Site selection results of coordinated planning

As shown in Fig. 5, the obtained planning scheme configured the ESS and VSC1 at node 0 and VSC2 at node 21. The length of the DC line was 0.4 km. The capacity of each VSC was 78 kVA, and the capacity of the ESS was 1101 kWh.

The planning results were compared with those of similar planning methods to highlight the advantages of the coordinated planning method. The results are shown in Table 3. Scheme 1 adopted only the ESS configuration. Scheme 2 adopted only flexible interconnections. Scheme 3 was the proposed planning method.

Table 3 Planning results of three schemes

Scheme	PV curtailment power capacity/ MWh	Operation and maintenance cost/ 10^3 yuan	Investment cost/ 10^3 yuan	Comprehensive cost/ 10^3 yuan
1	0	87.3	1004.3	1091.7
2	241.94	22.0	28.6	50.6
3	0	66.3	647.8	714.2

The results in Table 3 show that scheme 1 would achieve complete PV accommodation; however, the cost was relatively high, primarily because the investment cost of the ESS was high. The comprehensive cost of scheme 2 was low; however, the accommodation capacity of the PV system was limited. Owing to the high proportion of photovoltaic generation, the generated electricity surpassed the total power demand in both regions. Consequently, relying solely on flexible interconnected devices between areas could not achieve complete PV accommodation. Scheme 3 adopted coordinated planning for flexible interconnection devices and ESS, combining the respective advantages of ESS and flexible interconnection devices. Configuring the ESS would achieve complete PV accommodation and the low cost of the VSC ensured the economy of the planning results. Thus, scheme 3 achieved complete PV accommodation and a balance between the economy and PV accommodation.

The daily power curves of the VSC and ESS obtained from the optimization results are shown in Fig. 6.

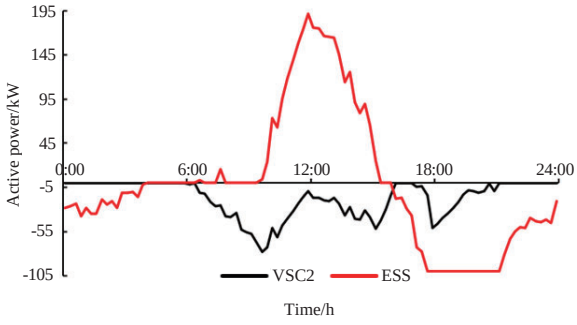

Fig. 6 Power curves of VSC2 and ESS

Fig. 6 shows that, first, during the onset of the reverse power in area 1, VSC2 transmitted the power of area 1 as much power as possible to area 2. Second, during the peak period of PV generation, both VSC2 and the ESS were optimized. VSC2 transmitted some of the reverse power to area 2, and the ESS stored the remaining reverse power, significantly improving the accommodation capacity of the PV. Finally, at night, the ESS discharged power, and VSC2 utilized the power complementarity to alleviate the overload problem of the distribution transformer in area 2.

Overall, the effectiveness of the proposed planning method was validated through an actual LVDN scenario, which verified its advantages in enhancing the PV accommodation capacity. The load ratio of a distribution transformer with an overload problem decreased to 0.7 or below through coordinated planning. Under the constraint of not permitting reverse power to be transmitted from the

LVDN to the MVDN, the PV accommodation rate increased to 100% through coordinated planning. Therefore, the coordinated planning of flexible interconnection devices and ESS effectively enhanced the accommodation capacity of PV, ensuring the safe operation of distribution transformers. The low cost of the VSC guaranteed economic feasibility of the planning results.

4.3 Coordinated planning results under different interconnection topologies

Different interconnection topologies have different effects on planning results. The various installation positions of the flexible equipment dictate the corresponding interconnection positions, thereby affecting the variations in the system topology and power flow distribution. This section analyses the corresponding planning results under different interconnection topologies and compares their economic costs. The decision variables were the installation location and capacity of the ESS and the capacities of the VSCs. Six typical interconnection topologies are shown in Fig. 7. When the PV penetration rate in area 1 exceeded 147.4%, a voltage violation occurred. To analyze the voltage violation and overload problems of distribution transformers in adjacent distribution areas, we increased the PV penetration rate to 176.2%.

The results of the network loss and selection of ESS locations are presented in Table 4. In the VSC capacity results for interconnection topology 6, the value 84 indicates the respective capacities of VSC1 and VSC2, and 23 represents the capacities of VSC3 and VSC4.

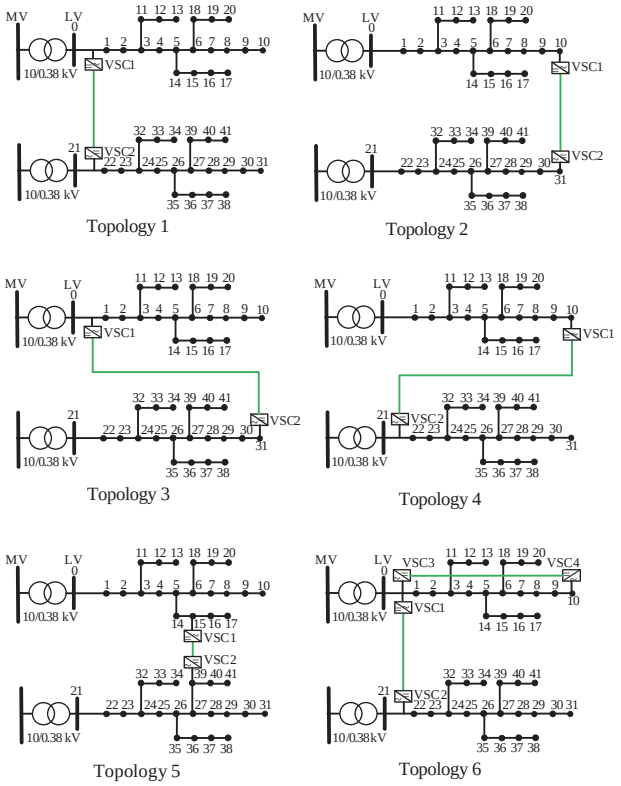

Fig. 7 Six typical interconnection topologies

Table 4 Results of allocation scheme and network loss

Mode	ESS's site selection results	ESS's capacity/ kWh	Single capacity of VSC/kVA	Daily network loss/kWh
1	Node 1	1484	84	207.32
2	Node 8	1500	84	183.98
3	Node 1	1484	84	200.04
4	Node 8	1500	84	198.93
5	Node 17	1507	83	182.68
6	Node 0	1486	84, 23	214.60

After planning, the total PV curtailment capacity for all interconnection topologies was zero. The various costs are listed in Table 5.

Table 5 Annual cost of various interconnection topologies

Mode	Investment of ESS/ 10^3 yuan	Operation and maintenance cost/10^3 yuan	Investment cost/ 10^3 yuan	Compre-hensive cost/ 10^3 yuan
1	834.4	82.3	864.6	946.9
2	843.4	82.5	874.0	956.5
3	834.4	80.9	869.9	950.8
4	843.4	85.5	879.0	964.5
5	847.4	82.4	876.9	959.4
6	835.6	83.8	877.0	960.8

Table 5 shows that interconnection topology 1 had the lowest annual comprehensive cost among the six interconnection topologies. The investment cost of the ESS constituted a large proportion, and the investment cost of ESS for interconnection topology 1 was the lowest. The lower maintenance cost of this topology was attributed to the proximity of the ESS to the distribution transformer. Although the network loss of interconnection topology 1 was high, the annual operational and maintenance costs were relatively low. Interconnection topology 5 exhibited the lowest network loss. Owing to the constraint that prevents reverse power flow from the LVDN to the MVDN, the increased ESS capacity in interconnection topology 5 resulted in higher annual comprehensive costs than topology

1. In addition, interconnection topology 6 adopted a parallel-connection scheme within the distribution area. This topology required a new set of VSC equipment, resulting in increased investment costs for VSCs and the DC line. Additionally, its network losses were the highest, resulting in higher operation, maintenance, and investment costs than interconnection topology 1. In conclusion, considering all these aspects, the economy of interconnection between the front nodes was optimal.

The voltage curves of all nodes in area 1 before planning are shown in Fig. 8. After optimization, the voltage curves under various interconnection topologies are shown in Fig. 9, indicating the voltages of all the nodes in a day.

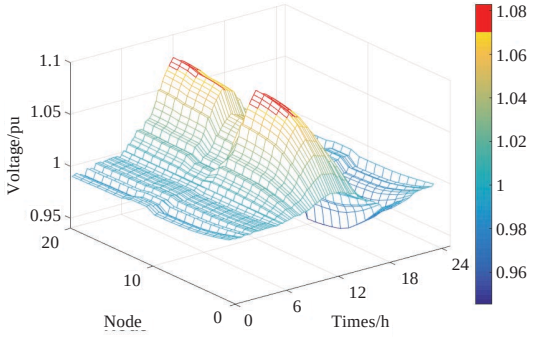

Fig. 8 Voltage curves of all nodes in area 1 before planning

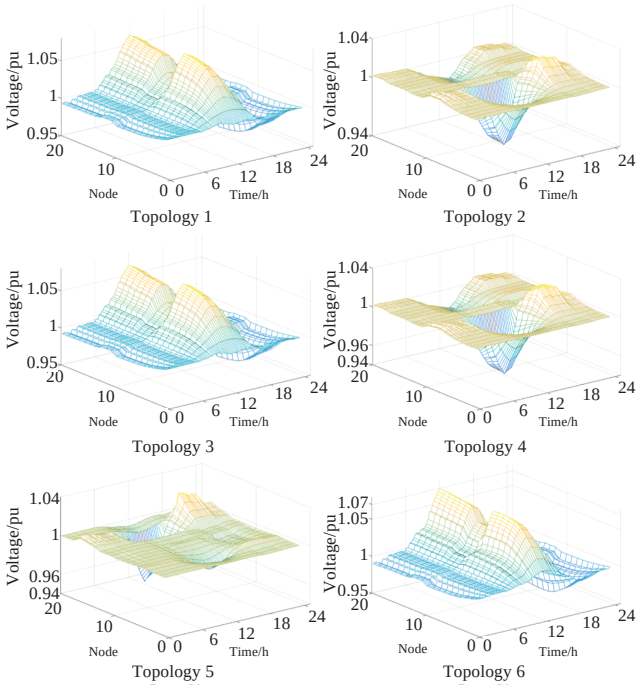

Fig. 9 Voltage curves after planning

Overall, the load rate of the distribution transformer with an overload problem was reduced to 0.7 or lower through coordinated planning, and the voltage violation problem was alleviated. Under the premise of not allowing a reverse power flow from the LVDN to the MVDN, coordinated planning increased the PV accommodation capacity to 100%. In addition, the differences in installation and maintenance costs for different installation locations were fully considered. The maintenance cost was low because the ESS site selection in interconnection topology 1 was similar to that of the distribution transformer. Although the network loss was high, the annual operation and maintenance costs were relatively low. Finally, we concluded that under a high penetration rate and decentralized integration of PV, the economy of adopting interconnection between front nodes was optimal.

4.4 Coordinated planning results under different PV grid-connected forms

Grid-connected PV forms can be divided into decentralized and centralized integration, and the results of coordinated planning vary under different grid-connected PV forms. This section analyzes the results of coordinated planning under different grid-connected PV forms and compares their economic costs and flexible interconnection topologies. The decision variables were the installation locations and capacities of the VSCs and ESS.

The planning results under decentralized integration are presented in Section 4.2, with a daily network loss of 175.56 kWh. The remaining experiments are not discussed.

Under centralized integration, the PV penetration rate in area 1 was the same as mentioned in Section 4.2. Given the practical engineering context, the available space at the front and terminal nodes was larger than that at other nodes, making them more suitable for centralized integration. Therefore, this section analyzes two options for centralized integration: front node zero and terminal node ten. After planning, the total PV curtailment capacity was reduced to 0. The results for the locations of the VSCs and ESS are shown in Fig. 10, and the allocation outcomes are listed in Table 6.

Table 6 Results of allocation scheme and network loss

PV's centralized integration point	ESS capacity/ kWh	VSC capacity/ kVA	DC line length/ km	Daily network loss/kWh
0	1060	78	0.4	196.69
10	1024	76	0.372	207.12

The cost outcomes of the centralized integration are listed in Table 7. When comparing the results with those of decentralized integration, we observed that the annual

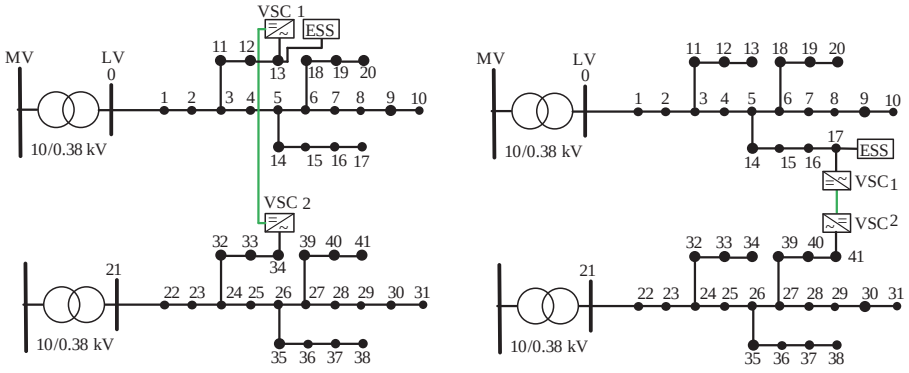

Node 0 install PVs　　Node 10 install PVs

Fig. 10　Site selection results of coordinated planning

Table 7　Various annual costs

PV integration point	Investment of ESS/ 10^3 yuan	Operation and maintenance cost/ 10^3 yuan	Investment cost/ 10^3 yuan	Comprehensive cost/ 10^3 yuan
0	596.1	74.1	625.2	699.3
10	575.8	75.0	603.8	678.8

comprehensive cost was lower in the centralized integration. Compared with centralized PV integration at the front node, network loss under centralized PV integration at the terminal node was higher, resulting in higher annual operation and maintenance costs. However, its annual ESS investment was relatively low; therefore, the economy of centralized PV integration into terminal nodes was better.

Meanwhile, the results of the flexible interconnection topologies for the two grid-connected PV forms were different. The interconnections between the front nodes are suitable for decentralized integration, which was consistent with the results presented in Section 4.3. This was primarily because, under this interconnection topology, the annual ESS investment cost was the lowest. Similarly, the interconnections between intermediate nodes were suitable for centralized integration.

5 Conclusion

To enhance the accommodation capacity of PV and mitigate the overload problem of distribution transformers and voltage violations in LVDN, this paper establishes a bilevel programming model with two objective functions. The model considers the variations in investment costs for different interconnected locations and differences in maintenance costs for newly added equipment at different locations. The rationality of the proposed coordinated planning method was validated through a comparative analysis of the three planning methods.

This paper analyzes the economic costs of planning schemes under various flexible interconnection topologies in the context of high PV penetration and decentralized integration. The site selection result of the ESS with the interconnection between the front nodes is close to that of the distribution transformer, resulting in lower maintenance costs. Despite the high network loss, the annual operation and maintenance costs are relatively low. After a comprehensive comparison, the economy of the interconnection between the front nodes was observed to be optimal. Finally, a comparative analysis was conducted on the planning results across different grid-connected PV forms, revealing that the optimal flexible interconnection topologies for the two different grid-connected PV forms differed. The coordinated planning method proposed in this paper has broad applicability and may improve PV accommodation and mitigate power supply quality problems.

Acknowledgements

This work was supported by the Science and Technology Support Program of Guizhou Province ([2022] General 012) and the Key Science and Technology Project of China Southern Power Grid Corporation (GZKJXM20220043).

Declaration of Competing Interest

We declare that we have no conflict of interest.

References

[1] Nour A, Helal A, Elsaadawi M, et al. (2020) Voltage violation in four-wire distribution networks integrated with rooftop PV systems. IET Renewable Power Generation, 14(13): 2395-2405

[2] Hraiz M D, García J A M, Castañeda R J, et al. (2020) Optimal PV size and location to reduce active power losses while achieving very high penetration level with improvement in voltage profile using modified Jaya algorithm. IEEE Journal of Photovoltaics, 10(4): 1166-1174

[3] Wang P, Liang F, Song J, et al. (2022) Impact of the PV location in distribution networks on network power losses and voltage fluctuations with PSO analysis. CSEE Journal of Power and Energy Systems, 8(2): 523-534

[4] Hoang P H, Ozkan G, Badr P R, et al. (2022) A dual distributed optimal energy management method for distribution grids with electric vehicles. IEEE Transactions on Intelligent Transportation Systems, 23(8): 13666-13677

[5] Moghaddass R, Mohammed O A, Skordilis E, et al. (2019) Smart control of fleets of electric vehicles in smart and connected communities. IEEE Transactions on Smart Grid, 10(6): 6883-6897

[6] Reshikeshan S S M, Matthiesen S L, Illindala M S, et al. (2021) Autonomous voltage regulation by distributed PV inverters with minimal inter-node interference. IEEE Transactions on Industry Applications, 57(3): 2058-2066

[7] Zeraati M, Golshan M E H, Guerrero J M (2019) Voltage quality improvement in low voltage distribution networks using reactive power capability of single-phase PV inverters. IEEE Transactions on Smart Grid, 10(5): 5057-5065

[8] Zhang T, Wang C, Luo F, et al. (2019) Optimal design of the sectional switch and tie line for the distribution network based on the fault incidence matrix. IEEE Transactions on Power Systems, 34(6): 4869-4879

[9] Zhang G, Wang Y, Peng B, et al. (2019) Multi-objective operation optimization of active distribution network based on three-terminal flexible multi-state switch. Journal of Renewable and Sustainable Energy, 11: 025501

[10] Wang X, Yang W, Liang D (2021) Multi-objective robust optimization of hybrid AC/DC distribution networks considering flexible interconnection devices. IEEE Access, 9: 166048-166057

[11] Baghban N S, Golshannavaz S, Nazarpour D, et al. (2019) Flexible feeder interconnections for increased penetration of renewables and improved volt/VAr control in distribution networks. IET Generation, Transmission & Distribution, 13(21): 4861-4869

[12] Zhang B, Li J, Zhang L, et al. (2023) Local control method and simulation analysis of hybrid AC/DC low-voltage distribution networks with high-proportion photovoltaics. Energy Reports, 9(7): 819-828

[13] Mudaliyar S, Mishra S (2021) Real-time coordinated control of low-voltage DC distribution network with soft opening point. IEEE Transactions on Power Electronics, 36(6): 7123-7137

[14] Zu G, Hao Z, Huang X, et al. (2023) Maximum power supply capacity of distribution network considering flexible interconnection in low-voltage station area. Automation of Electric Power System, 47(07): 84-93

[15] Zhang L, Tong B, Wang Z, et al. (2022) Optimal configuration of hybrid AC/DC distribution network considering the temporal power flow complementarity on lines. IEEE Transactions on Smart Grid, 13(5): 3857-3866

[16] Newton C, Lang P, Terry S (2017) Field trial results of power electronics in low-voltage distribution networks. CIRED Open Access Proceedings Journal, 2017(1): 184-188

[17] Xu Y, Liu H, Xiong X, et al. (2022) Key technologies and development modes of flexible interconnection of low-voltage distribution station area. Proceedings of the CSEE, 42(11): 3986-4001

[18] Li X, Wang L, Yan N, et al. (2021) Cooperative dispatch of distributed energy storage in distribution network with PV generation systems. IEEE Transactions on Applied Superconductivity, 31(8): 0604304

[19] Guo Z, Zhang X, Li M, et al. (2022) Control and capacity planning for energy storage systems to enhance the stability of renewable generation under weak grids. IET Renewable Power Generation, 16(4): 761-780

[20] Giglio E, Luzzani G, Terranova V, et al. (2023) An efficient artificial intelligence energy management system for urban building integrating photovoltaic and storage. IEEE Access, 11: 18673-18688

[21] Golpîra H, Messina A R, Bevrani H (2019) Emulation of virtual inertia to accommodate higher penetration levels of distributed generation in power grids. IEEE Transactions on Power Systems, 34(5): 3384-3394

[22] Tong L, Zhao S, Jiang H, et al. (2021) Multi-scenario and multi-objective collaborative optimization of distribution network considering electric vehicles and mobile energy storage systems. IEEE Access, 9: 55690-55697

[23] Li Q, Ayyanar R, Vittal V (2016) Convex optimization for DES planning and operation in radial distribution systems with high penetration of photovoltaic resources. IEEE Transactions on Sustainable Energy, 7(3): 985-995

[24] Iba K (2022) Massive energy storage system for effective usage of renewable energy. Global Energy Interconnection, 5(3): 301-308

[25] Li C, Yan J, Sun D, et al. (2022) Multidimensional economic evaluation of energy storage participation in multiple scenarios in distribution networks. Global Energy Interconnection, 5(5): 471-479

[26] Zhang L, Xu B, Tang W, et al. (2021) Intra-day correction strategy of dispatching plan for AC/DC hybrid distribution network based on spatio-temporal power coordination. Automation of Electric Power System, 45(24): 106-114

[27] Ding Z, Huang X, Liu Z, et al. (2022) A two-level scheduling algorithm for battery systems and load tap changers coordination in distribution networks. IEEE Transactions on Power Delivery, 37(4): 3027-3037

[28] Ning K, Liu J, Zhang C, et al. (2023) Collaborative planning of energy storage and DC site selection and capacity determination in distribution networks considering photovoltaic consumption. Global Energy Interconnection, 6(1): 45-53

[29] Ahmed H M A, Eltantawy A B, Salama M M A (2018) A planning approach for the network configuration of AC-DC

hybrid distribution systems. IEEE Transactions on Smart Grid, 9(3): 2203-2213

[30] Beerten J, Cole S, Belmans R (2012) Generalized steady-state VSC MTDC model for sequential AC/DC power flow algorithms. IEEE Transactions on Power Systems, 27(2): 821-829

[31] Mehdi Z, Mohamadesmail H G, Josepm G (2018) Distributed control of battery energy storage systems for voltage regulation in distribution networks with high PV penetration. IEEE Transactions on Smart Grid, 9(4): 3582-3593

[32] Liu Y, Yu Z, Li H, et al. (2019) The LCOE-indicator-based comprehensive economic comparison between AC and DC power distribution networks with high penetration of renewable energy. Energies, 12(24): 4621

[33] Zhong W (2015) Analysis of ways to improve the maintenance efficiency of electrical equipment. Decision Forum, 8: 15

[34] Liu Y, Li T, Wang X, et al. (2021) Research on differentiated input of operation and maintenance cost based on different power grid equipment states. Paper presented at 2021 IEEE 2nd China International Youth Conference on Electrical Engineering (CIYCEE), Chengdu, China, 15-17 December 2021

Biographies

Jiaguo Li (Student Member, IEEE) was born in Jiangsu, China on February, 1994. He received the B.S. degree in electrical engineering from Northeast Electric Power University, Jilin, China, in 2018. He is currently pursuing the M.S. degree in electrical engineering at the College of Information and Electrical Engineering of China Agricultural University, Beijing, China. His main research fields are Power system operation and planning.

Lu Zhang (Member, IEEE) was born in Beijing, China on February 10, 1990. He received the B.S. degree in electrical engineering and the Ph.D. degree in Agricultural Electrification and Automation from China Agricultural University, Beijing, China, in 2011 and 2016, respectively. He was a postdoc in the Department of Electrical Engineering at Tsinghua University From 2017 to 2019. He is currently an Associate Professor at College of Information and Electrical Engineering, China Agricultural University, Beijing, China. His main research interests include hybrid AC/DC distribution network, renewable energy generation, and active distribution networks.

Bo Zhang (Member, IEEE) received the B.S. degree in electrical engineering in 2016 from China Agricultural University, Beijing, China, where she is currently working toward the Ph.D. degree in agricultural electrification and automation with the College of Information and Electrical Engineering. Her main research interests include hybrid AC/DC distribution network, renewable energy generation, and economic operation of active distribution network.

Wei Tang (Member, IEEE) received the B.S. degree in electrical engineering from Huazhong University of Science and Technology, Wuhan, China, in 1992 and the Ph.D. degree in electrical engineering from Harbin Institute of Technology, Harbin, China, in 1998. From 1998 to 2000, she was a post-doctor with Harbin Engineering University. She is currently a professor at the College of Information and Electrical Engineering, China Agricultural University, Beijing, China. Her research interests include distribution network economic and security operation, distributed generation and active distribution network.

(Editor Yajun Zou)